Multi-scale analysis of well-logs and of seismic reflection data

C.P.A. Wapenaar, J.C.M. Goudswaard, W.J.F. van Geloven and J.T. Fokkema,
Centre for Technical Geoscience, Delft Univ. of Technology

Summary

In well-logs we often encounter sharp outliers, or singularities, that are responsible for strong reflections. However, these reflectors are different from step-functions, in the sense that step-functions are scale-invariant whereas these singularities are not. In this paper a multi-scale analysis has been performed on synthetic and real well-logs, as well as on their reflection responses, in order to test a method that can distinguish between scale-invariant and scale-variant reflectors. We will show that it is possible to extract a stable local singularity exponent α from a well-log, and that we can obtain the same exponent from seismic reflection data.

Introduction

Multi-scale analysis is usually performed on well-logs; only recently this analysis is being applied to seismic data [1]. In this paper we investigate media that contain different types of singularities. If singularities are described in a self-similar way, it can be proven that, except for the step-function, they are scale-variant. This implies that the angle-dependent seismic reflection response is scale-variant as well, in a way that is directly linked to the scaling behavior of the well-log. In this paper we will show how to extract a local singularity exponent both from the well-log as well as from the seismic reflection data. In the first example we consider a synthetic well-log with well-defined self-similar singularities, in the second example the singularities will be taken from real well-logs.

A model for a scale-variant singularities

In this paper we consider singularities of the form

$$c(z) = \begin{cases} c_1 |z/z_1|^{\alpha} & \text{for } z < 0 \\ c_2 |z/z_2|^{\alpha} & \text{for } z > 0. \end{cases} \tag{1}$$

Figure 1a shows a synthetic well-log that consists of three such singularities, with $\alpha = -0.4$, $\alpha = 0$ and $\alpha = 0.2$, respectively. Note that for $\alpha = 0$ the singularity reduces to a step-function. Moreover, for arbitrary α the singularities are *self-similar*, according to

$$c(\beta z) = \beta^{\alpha} c(z) \quad \text{for} \quad \beta > 0, \tag{2}$$

see Figure 2. This property will be exploited in the analysis of the multi-scale AVA behavior of the reflection response of these singularities. But first we analyze the multi-scale behavior of the singularities themselves.

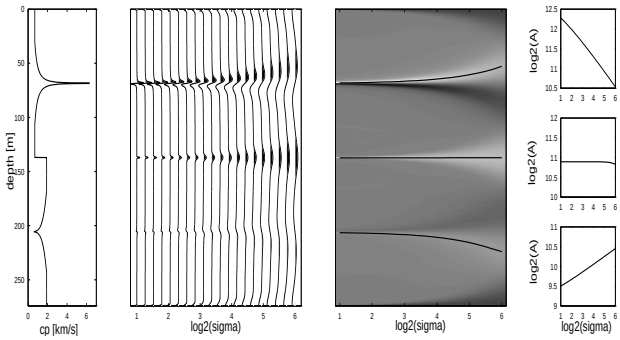

(a) (b) (c) (d)

Fig. 1: *(a) Synthetic well-log. (b) Wavelet transform of the well-log. (c) Position of modulus-maxima lines in wavelet transform. (d) Log-log plot of amplitude along modulus-maxima lines vs. scale: (top) $\alpha = -0.4$, (middle) $\alpha = 0$, (bottom) $\alpha = 0.2$.*

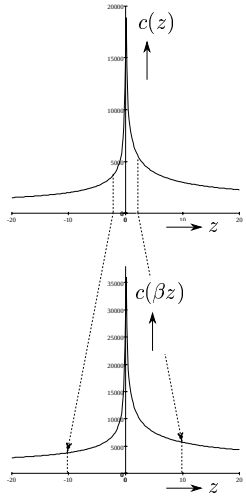

Fig. 2: *The self-similar singularity $c(z)$ of equation (1), with $\alpha = -0.4$, $c_1 = 2000$ m/s, $c_2 = 3000$ m/s, $z_1 = z_2 = 10$ m. The "zoom-factor" is chosen as $\beta = 0.2$, hence, the scaling factor β^{α} in equation (2) equals 1.904.*

Multi-scale analysis of the singularities

The following analysis is due to Mallat and Hwang [3] and has been applied to well-logs by Herrmann [2]. Let the wavelet transform $\check{c}(\sigma, z)$ of $c(z)$ be defined as

$$\check{c}(\sigma, z) = \frac{1}{\sigma} \int_{-\infty}^{\infty} c(z') \psi\Big(\frac{z' - z}{\sigma}\Big) \mathrm{d}z', \quad (\sigma > 0), \tag{3}$$

with $\psi(z)$ being a proper analyzing wavelet and σ the scale parameter. For the well-log of Figure 1a, the wavelet transform $\check{c}(\sigma, z)$ is shown in Figure 1b.

Replacing z' by $\sigma z'$, $\mathrm{d}z'$ by $\sigma \mathrm{d}z'$ and substituting equation (2) yields

$$\check{c}(\sigma, z) = \sigma^{\alpha} \int_{-\infty}^{\infty} c(z')\psi(z' - z/\sigma)\mathrm{d}z', \qquad (4)$$

or, comparing the right-hand side with that of equation (3),

$$\check{c}(\sigma, z) = \sigma^{\alpha}\check{c}(1, z/\sigma). \qquad (5)$$

Let $z = z_{\max}$ denote the z-value for which $|\check{c}(\sigma, z)|$ reaches a local maximum for a fixed scale σ. Mallat and Hwang [3] define a *modulus maxima line* as the curve in the (σ, z)-plane that connects the local maxima $|\check{c}(\sigma, z_{\max})|$ for all σ, see Figure 1c. From equation (5) it follows that the logarithm of the amplitude along a modulus maxima line is given by

$$\log|\check{c}(\sigma, z_{\max})| = \alpha \log\sigma + \log|\check{c}(1, z_{\max}/\sigma)|, \qquad (6)$$

see Figure 1d. It appears that the slope of this modulus maxima function is equal to the local singularity exponent α. Herrmann [2] has applied this type of multi-scale analysis to real well-logs. His results show that the modulus maxima functions of many singularities in well-logs exhibit a constant α behavior (as in Figure 1d) over a wide range of scales.

Multi-scale AVA analysis of the reflection response

Figure 3a shows the plane wave response of the well-log of Figure 1a in the ray-parameter intercept-time (p, τ) domain as well as an image in the ray-parameter depth (p, z) domain. Note that this reflection response, which is modeled by a reflectivity method, has been convolved with a (symmetrical) wavelet, to represent the data in a more comfortable way.

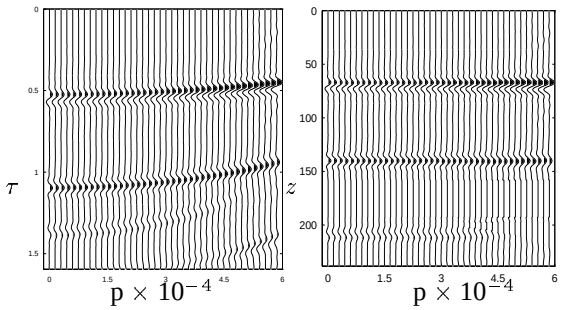

Fig. 3: *(a) Plane wave response (p, τ-domain) of synthetic well-log. (b) Imaged plane wave response (p, z-domain).*

In this section we will derive the multi-scale AVA-behavior of this reflection response. Our starting point is the wave equation in the (p, τ)-domain, with $c(z)$ defined by equation (1):

$$\left[\frac{\partial^2}{\partial z^2} - \Big(\frac{1}{c^2(z)} - p^2\Big)\frac{\partial^2}{\partial \tau^2}\right] u(z, p, \tau) = 0. \qquad (7)$$

Replacing z by βz, substituting equation (2) and multiplying the result by β^2 gives

$$\left[\frac{\partial^2}{\partial z^2} - \Big(\frac{1}{c^2(z)} - (\beta^{\alpha}p)^2\Big)\frac{\partial^2}{(\partial \beta^{\alpha-1}\tau)^2}\right] u(\beta z, p, \tau) = 0. \qquad (8)$$

The term between the square brackets is the same as in equation (7), with p replaced by $\beta^{\alpha}p$ and τ replaced by $\beta^{\alpha-1}\tau$. Hence, equation (8) is satisfied by $u(z, \beta^{\alpha}p, \beta^{\alpha-1}\tau)$ as well as $u(\beta z, p, \tau)$. Consequently,

$$u(z, \beta^{\alpha}p, \beta^{\alpha-1}\tau) = f(\alpha)u(\beta z, p, \tau), \qquad (9)$$

where $f(\alpha)$ is an undetermined α-dependent factor. In the upper half-space $z < 0$ we define an 'incident' wave field u^{inc} (with positive power flux) and a 'reflected' wave field u^{refl} (with negative power flux), both obeying equation (9) with one and the same factor $f(\alpha)$. For our analysis we do not need to specify this 'decomposition' any further. We relate these incident and reflected wave fields via a reflection kernel $r(p, \tau)$, according to

$$u^{\mathrm{refl}}(-\epsilon, p, \tau) = \int_{-\infty}^{\infty} r(p, \tau - \tau')u^{\mathrm{inc}}(-\epsilon, p, \tau')\mathrm{d}\tau', \qquad (10)$$

with $\epsilon \to 0$. Replacing ϵ by $\beta\epsilon$, substituting equation (9) for u^{inc} and u^{refl} and comparing the result with equation (10) learns that the reflection kernel obeys the following similarity relation

$$r(p, \tau) = \beta^{\alpha-1} r(\beta^{\alpha}p, \beta^{\alpha-1}\tau). \qquad (11)$$

We introduce the wavelet transform of $r(p, \tau)$ by

$$\check{r}(p, \sigma, \tau) = \int_{-\infty}^{\infty} r(p, \tau')\psi\Big(\frac{\tau' - \tau}{\sigma}\Big)\mathrm{d}\tau'. \qquad (12)$$

Substituting equation (11), replacing τ' by $\beta^{1-\alpha}\tau'$ and $\mathrm{d}\tau'$ by $\beta^{1-\alpha}\mathrm{d}\tau'$ yields

$$\check{r}(p, \sigma, \tau) = \int_{-\infty}^{\infty} r(\beta^{\alpha}p, \tau')\psi\Big(\frac{\tau' - \beta^{\alpha-1}\tau}{\beta^{\alpha-1}\sigma}\Big)\mathrm{d}\tau', \qquad (13)$$

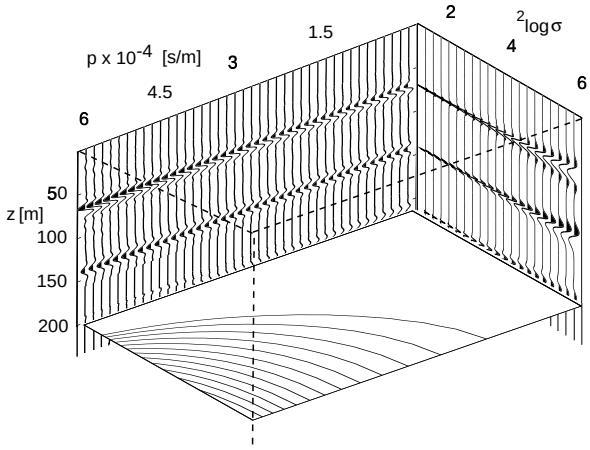

Fig. 4: *Multi-scale representation $\check{r}(p, \sigma, z)$ of the imaged seismic data of Figure 3b.*

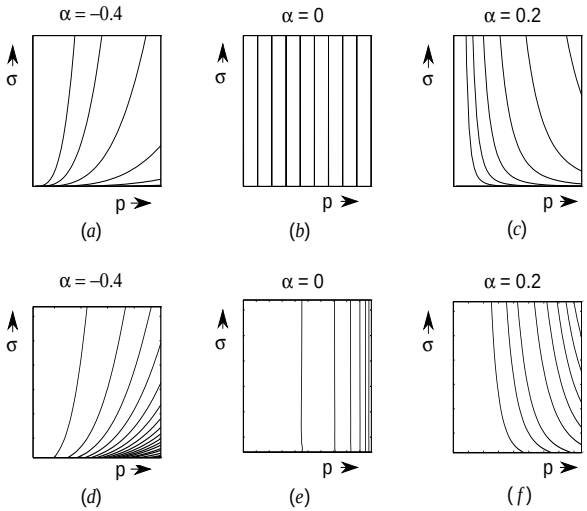

Fig. 5: *Analytical contours along which $p^{1-\alpha}\sigma^{\alpha}$ =constant: (a) $\alpha = -0.4$, (b) $\alpha = 0$, (c) $\alpha = 0.2$. The corresponding results obtained from the multi-scale image in Figure 4 are shown in (d), (e) and (f)*

or, comparing the right-hand side with that of equation (12),

$$\check{r}(p, \sigma, \tau) = \check{r}(\beta^{\alpha} p, \beta^{\alpha-1}\sigma, \beta^{\alpha-1}\tau). \qquad (14)$$

Let $\tau = \tau_{\max}$ denote the τ-value for which $|\check{r}(p, \sigma, \tau)|$ reaches its maximum for fixed p and σ. We define a *modulus maxima plane* as the plane in the (p, σ, τ)-space that connects the local maxima $|\check{r}(p, \sigma, \tau_{\max})|$ for all p and σ. It follows from equation (14) that the reflection amplitude in a modulus maxima plane behaves as

$$|\check{r}(p, \sigma, \tau_{\max})| = |\check{r}(\beta^{\alpha} p, \beta^{\alpha-1}\sigma, \beta^{\alpha-1}\tau_{\max})|. \qquad (15)$$

The latter equation implies that contours of constant reflection amplitude in a modulus maxima plane are described by

$$p^{1-\alpha}\sigma^{\alpha} = \text{constant}. \qquad (16)$$

The same contours of constant reflection amplitude $|\check{r}(p, \sigma, z_{\max})|$ are found in the modulus maxima planes of the imaged reflection data, see Figures 4 and 5.

Examples on a real velocity well-log

The aforementioned method has been performed on certain strong reflectors in an actual sonic P-velocity log. In the first example a piece of a log (Figure 6a) has been chosen of 1500 samples (i.e. 250 m) in which the acoustic reflection response was modeled. Making use of the multi-scale analysis a reflector was found at a depth of around 160m with a constant singularity exponent α=-0.32 (see Figure 6b), in the $^2\log\sigma$-range [2,5]. This scale range is approximately equal to a wavelength of 8 to 60 m, which corresponds to the higher frequencies in the seismic spectrum. The imaged reflection response is visible in Figure 6c. As we have used the same sampling for the velocity function as for the imaging, we can state that the scales in all pictures are directly comparable. We can see that there is a strong reflector which corresponds to the one already pointed out. At this depth level a wavelet transform has been performed and we have measured the amplitude of the envelope of the reflectivity along *modulus maxima* planes. The result of this analysis is given in Figure 6d. Using equation (16) we derived from these curves $\alpha \approx -0.34$, which is quite close to the value derived from the well-log. We have also performed the method on a log in which a step-function was present ($\alpha \approx 0$). This log, which is visible in Figure 7a, contains this step-function at a depth of about 90 m. The results of the multi-scale analysis are shown in Figure 7b. We can clearly see that the singularity exponent is approximately equal to 0 for the logarithmic scale range [2,5]. Just as in the foregoing case, the imaged reflection response is given in Figure 7c, and the value of the reflectivity along the modulus maxima planes has been given in Figure 7d. In this picture we can clearly see that the pattern is different from Figure 6d. If we compare these curves with the analytical curves in Figure 5a,b,c, we can see that the trend of the curves is best represented by a value of $\alpha = 0$.

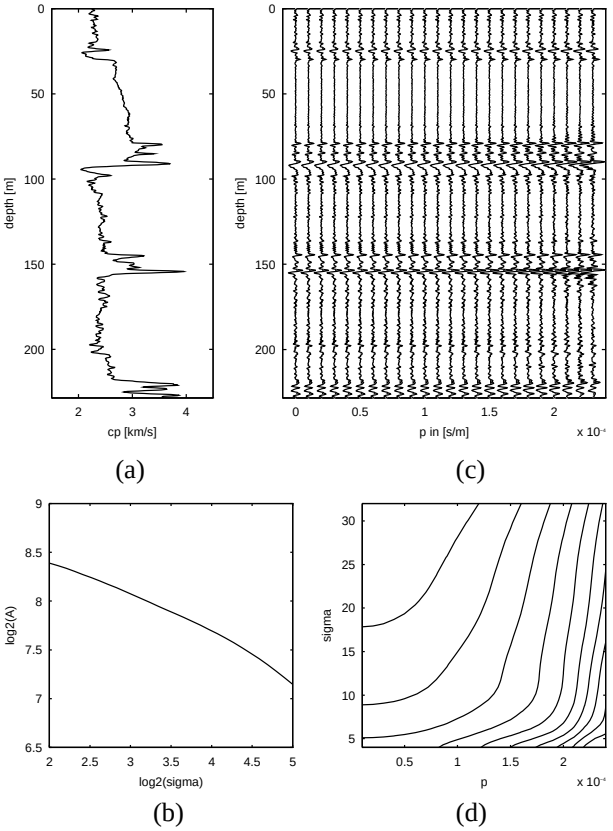

Fig. 6: *(a) Velocity function as used in this example. (b) Log-log plot of amplitude along modulus-maxima lines vs. scale at a depth of around 160 m (slope $\alpha \approx -0.32$). (c) Imaged reflection response of this velocity function. (d) $|\check{r}(p, \sigma, z_{max})|$ in a modulus maxima plane at the same depth as the analysis in (b).*

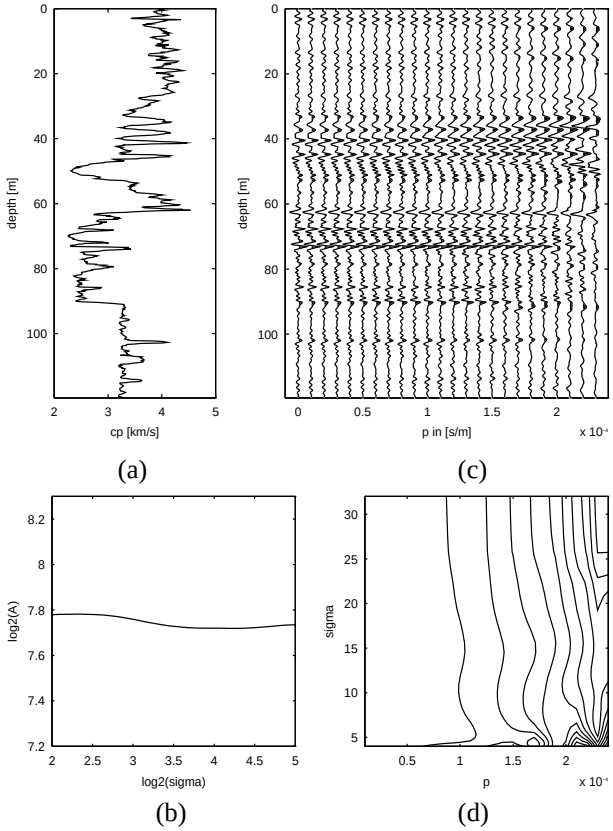

Fig. 7: *(a) Velocity function as used in this example. (b) Log-log plot of amplitude along modulus-maxima lines vs. scale at a depth of around 90 m (slope $\alpha \approx 0$). (c) Imaged reflection response of this velocity function. (d) $|\check{r}(p, \sigma, z_{max})|$ in a modulus maxima plane at the same depth as the analysis in (b).*

Conclusion and discussion

We have shown that it is possible to retrieve a scale parameter from the reflection response of a medium, which is consistent with the one derived from a sonic velocity log, in the same scale range. Up till now, the method has not been tested on real reflection data.

Note that we only used local *amplitude* information (retrieved from modulus maxima planes), to estimate the singularity exponent. We will investigate the possibility to include local *phase* information as well, in order to obtain more stable estimates of the local singularity exponent.

When looking at the results obtained from seismic data modeled in the real well-logs, we expect that the singularity exponent α may prove to be a useful seismic indicator, in addition to other parameters in AVA inversion.

Acknowledgement

The authors would like to thank the Dutch Technology Foundation (STW) for their financial support.

References

[1] F. J. Dessing, E. V. Hoekstra, F. J. Herrmann, and C. P. A. Wapenaar. Multiscale edge detection by means of multiscale migration. In *Soc. Expl. Geophys., Expanded Abstracts*, 1996.

[2] F. J. Herrmann. *A scaling medium representation*. PhD thesis, Delft University of Technology, 1997.

[3] S. G. Mallat and W. L. Hwang. Singularity detection and processing with wavelets. *IEEE Trans. Inform. Theory*, 38(2):617–643, 1992.